


Loop-loop interactions involved in antisense regulation are processed by the endoribonuclease III in *Staphylococcus aureus*

Cédric Romilly, Clément Chevalier, Stefano Marzi, Benoît Masquida, Thomas Geissmann, François Vandenesch, Eric Westhof & Pascale Romby


To cite this article: Cédric Romilly, Clément Chevalier, Stefano Marzi, Benoît Masquida, Thomas Geissmann, François Vandenesch, Eric Westhof & Pascale Romby (2012) Loop-loop interactions involved in antisense regulation are processed by the endoribonuclease III in *Staphylococcus aureus*, *RNA Biology*, 9:12, 1461-1472, DOI: [10.4161/rna.22710](https://doi.org/10.4161/rna.22710)

To link to this article: <http://dx.doi.org/10.4161/rna.22710>

 View supplementary material 

 Published online: 07 Nov 2012.

 Submit your article to this journal 

 Article views: 275

 View related articles 

 Citing articles: 10 View citing articles 

Loop-loop interactions involved in antisense regulation are processed by the endoribonuclease III in *Staphylococcus aureus*

Cédric Romilly,^{1,†} Clément Chevalier,^{2,†} Stefano Marzi,¹ Benoit Masquida,¹ Thomas Geissmann,^{3,4} François Vandenesch,^{3,4,5} Eric Westhof¹ and Pascale Romby^{1,*}

¹Architecture et Réactivité de l'ARN; Université de Strasbourg; CNRS; Strasbourg, France; ²Department of Biology; ETH Zurich; Zurich, Switzerland;

³Université de Lyon; Lyon, France; ⁴Inserm U851; Lyon, France; ⁵Hospices Civils de Lyon; Lyon, France

[†]These authors contributed equally to this work.

Keywords: endoribonuclease, loop-loop interaction, gene regulation, regulatory RNA, processing

The endoribonuclease III (RNase III) belongs to the enzyme family known to process double-stranded RNAs. *Staphylococcus aureus* RNase III was shown to regulate, in concert with the quorum sensing induced RNAIII, the degradation of several mRNAs encoding virulence factors and the transcriptional repressor of toxins Rot. Two of the mRNA-RNAIII complexes involve fully base paired loop-loop interactions with similar sequences that are cleaved by RNase III at a unique position. We show here that the sequence of the base pairs within the loop-loop interaction is not critical for RNase III cleavage, but that the co-axial stacking of three consecutive helices provides an ideal topology for RNase III recognition. In contrast, RNase III induces several strong cleavages in a regular helix, which carries a sequence similar to the loop-loop interaction. The introduction of a bulged loop that interrupts the regular helix restrains the number of cleavages. This work shows that *S. aureus* RNase III is able to bind and cleave a variety of RNA-mRNA substrates, and that specific structure elements direct the action of RNase III.

Introduction

The regulation of mRNA decay plays essential roles in the regulation of gene expression, enabling the bacteria to selectively activate or repress appropriate genes in response to a specific physiological state. This is particularly true for pathogenic bacteria such as *Staphylococcus aureus*, which can survive under extreme circumstances in the human host as well as in the environment. *S. aureus* is both a commensal bacterium and an opportunistic pathogen, which causes a wide variety of infections, owing in part to the coordinated expression of a large repertoire of virulence factors.^{1–3} Genome-wide studies have shown that the decay of mRNAs encoding virulence factors is highly regulated during growth.^{4,5} Furthermore, the stability of many transcripts is modified upon the entry into the stationary phase of growth and in response to various stresses.^{6,7} Detailed knowledge about the RNA decay machinery in *S. aureus* was recently gained.^{5,8} Indeed, the genome encodes all the orthologs of *Bacillus subtilis* exoribonucleases and endoribonucleases, suggesting that the mechanisms of RNA decay are conserved in Gram-positive bacteria.^{9,10} A two-hybrid system identified a degradosome-like complex composed of the two bi-functional RNases J1 and J2, the endoribonuclease Y, the 3'-5' exoribonuclease PNPase, enolase,

phosphofructokinase, the DEAD-box RNA helicase CshA and the protein subunit of RNase P, RnpA.⁹ Surprisingly, the essential protein RnpA is endowed with a ribonuclease activity and a small molecule inhibitor of RnpA-mediated RNA degradation has been recently selected, which exhibited antimicrobial activity against hypervirulent and multi-drug resistant *S. aureus* strains.¹¹ Thus, RNA degradation appears to be a cellular process that can be targeted by antimicrobial drugs. Two other endoribonucleases of *S. aureus*, RNase Y and RNase III, were shown to be essential for the full virulence of *S. aureus* in several murine models including bacteraemia,¹² intraperitoneal¹³ and peritonitis,¹⁴ although they are not essential for growth.^{12,14,15} Interestingly, both enzymes are important for the processing and stabilization of specific mRNAs, and contribute to the turnover of small non-coding RNAs.^{12,16}

RNase III is one of the extensively studied RNases in *S. aureus*. It belongs to the family of Mg²⁺-dependent endoribonucleases in eukaryotes and bacteria, which recognize and cleave double-stranded RNA (dsRNA) to generate a dsRNA with a 5' phosphate group and a two nucleotides 3'-overhang.¹⁷ Bacterial RNase III acts as an active homodimeric enzyme with each subunit carrying the catalytic activity and substrate recognition.¹⁸ We have previously shown that the biochemical properties of

*Correspondence to: Pascale Romby; Email: p.romby@ibmc-cnrs.unistra.fr
Submitted: 09/11/12; Revised: 10/25/12; Accepted: 10/29/12
<http://dx.doi.org/10.4161/rna.22710>

S. aureus RNase III are very similar to those of *Escherichia coli* RNase III. As for *E. coli*,^{19,20} conserved acidic residues and Mg²⁺ are essential for the cleavage reaction.^{16,21} *S. aureus* RNase III was first shown to act as a co-factor of the quorum-sensing regulatory RNAIII to irreversibly repress the synthesis of several adhesins and the transcriptional repressor of toxins, Rot.^{15,22–24} Moreover, a recent study discovered an antisense transcription all over the genome, which is hidden in *S. aureus* strains due to RNase III processing of sense/antisense transcripts.²⁵ Finally, a wide range of structured RNAs recognized by RNase III have been identified by in vivo immunoprecipitation of wild type or cleavage-defective mutant RNase III followed by deep sequencing.¹⁶ This study revealed that besides its universal function in rRNA maturation and RNA turnover, RNase III affects processing of mRNAs carrying overlapping 5'UTRs. Moreover, it directs maturation of mRNAs resulting in their stabilization and antisense regulation mediated by small RNAs.

We have previously shown that RNase III unexpectedly cleaved several RNAIII-mRNA complexes forming loop-loop interactions.^{23,24} Intriguingly, these short intermolecular base paired helices (7 to 8 nucleotides) share structure and sequence similarities and are a priori not considered as RNase III substrates. We demonstrate here that the sequence of these base pairs is not critical for cleavage but that the co-axial stacking of the newly formed intermolecular helices provides an ideal topology for RNase III recognition and cleavage. This work also shows that RNA-RNA complexes contain both positive and negative elements to limit and/or direct the action of RNase III, as it was previously demonstrated for *E. coli* RNase III.^{26,27}

Results

Design of the RNA substrates to be probed by RNase III cleavage assays. *S. aureus* RNAIII is a multi-functional RNA that encodes δ -hemolysin and regulates the synthesis of many virulence factors and enzymes involved in peptidoglycan metabolism at high cell density.^{3,24,28} We have previously shown that the large 3' UTR of RNAIII is acting as an antisense RNA (asRNA) to repress the translation of multiple mRNAs.^{15,23,24} This region contains three hairpin structures with a conserved C-rich sequence located in the apical loops, which serve as the seed sequence to initiate fast binding with G-rich sequences of mRNA targets.²⁴ Determination of the structures of several regulatory RNAIII-mRNA complexes revealed bi-partite binding sites that differed according to the mRNA structures: an imperfect duplex that sequestered the Shine and Dalgarno sequence (SD), was stabilized by a loop-loop interaction in the coding region of *coa* mRNA encoding coagulase (Fig. 1A), or two loop-loop interactions involving the 5' untranslated region and the SD sequence of *rot* mRNA that encoded the transcriptional repressor of toxins (Fig. 1A). These complexes prevent the formation of the initiation ribosomal complex and recruit RNase III to initiate the degradation of the repressed mRNAs. Interestingly, previous RNase III cleavage assays performed on 5' end-labeled mRNAs bound to RNAIII showed a single strong cleavage in *coa* and *rot* mRNAs located at an equivalent position of the loop-loop pairings^{23,24}

(Fig. 1A). In both systems, the sequence of the loop-loop interactions is highly similar although the length and sequences of the intramolecular helices are different (Fig. 1A). The same reaction was performed with 5' end-labeled RNAIII alone and in the presence of increasing concentrations of cold *coa* mRNA or *rot* mRNA (Fig. 1B). The data showed that binding of *coa* or of *rot* mRNA similarly induced an RNase III cleavage located in the hairpin loop H7 of RNAIII at C240 (Fig. 1). However, the two loop-loop interactions found in RNAIII-*rot* mRNA complex are not strictly equivalent because no cleavage was observed in the hairpin loop H14 of RNAIII (Fig. 1B).

Because the sequences involved in the kissing loops were very similar, we have analyzed whether the RNase III cleavage pattern resulted from a specific recognition of the base pairs or from the topology of the kissing complex. To distinguish between these two hypotheses, we have constructed several RNA substrates based on the kissing interactions as found in *coa* mRNA-RNAIII complex and have compared their RNase III cleavage patterns. The sequences of the kissing loops, i.e., loop III of *coa* mRNA and loop 7 of RNAIII, were changed so that the stability of the base pairs was not perturbed (Fig. 1A). Structure modeling of the kissing interaction has been previously completed revealing a co-axial stacking of the intramolecular and intermolecular helices to form a long helical structure.²⁴ Based on this model, we have superimposed a regular helix on the kissing complex to define the appropriate length of the helix for comparative RNase III probing. Two regular helices (30 and 33 base pairs) and a stem-loop structure of 30 base pairs (bp), mimicking the size of the long helical structure promoted by the kissing interactions, were chemically synthesized. Two last RNA constructs introducing a bulged loop were made to interrupt regular helices (irregular helices, Fig. 1C).

Changing the sequence of the loop-loop interaction has no effect on RNase III cleavage. We first verified that the nucleotide substitution in RNAIII and *coa* mRNA mutants (Fig. 1A) did not alter the RNA structure and/or binding. The secondary structures of wild type (WT) and mutant *coa* mRNAs were probed using RNase T1 (specific for unpaired guanines) and RNase V1 (specific for helical regions). The cleavages were mapped using 5' end-labeled mRNA and sized on a denaturing polyacrylamide gel (Fig. 2A). The data correlated well with the secondary structure of *coa* mRNA which was previously published²⁴ (Fig. 2A). Indeed, the main RNase T1 cleavages are located in the apical loops I and III and strong RNase V1 cuts occurred in helical regions of *coa* mRNA (Fig. 2B). In the mutant mRNA, the major changes occurred in loop III because the three guanines 94–96 have been substituted by cytosines. Binding of mutant RNAIII induced changes in the region encompassing the ribosome binding site (RBS, nucleotides U10 to A48) of the mutant *coa* mRNA, as it was shown for the WT RNAIII-mRNA complex. Mutant RNAIII protected the guanines (G19–20, G22–23) of the SD sequence against RNase T1, while new RNase V1 cleavages were observed at positions 39–41 of the mRNA (Fig. 2A). These data show that the mutant RNAIII binds to the RBS of the mutant *coa* mRNA in a manner similar to that of the WT RNAs. In addition, the WT RNAIII binding induced strong protection of

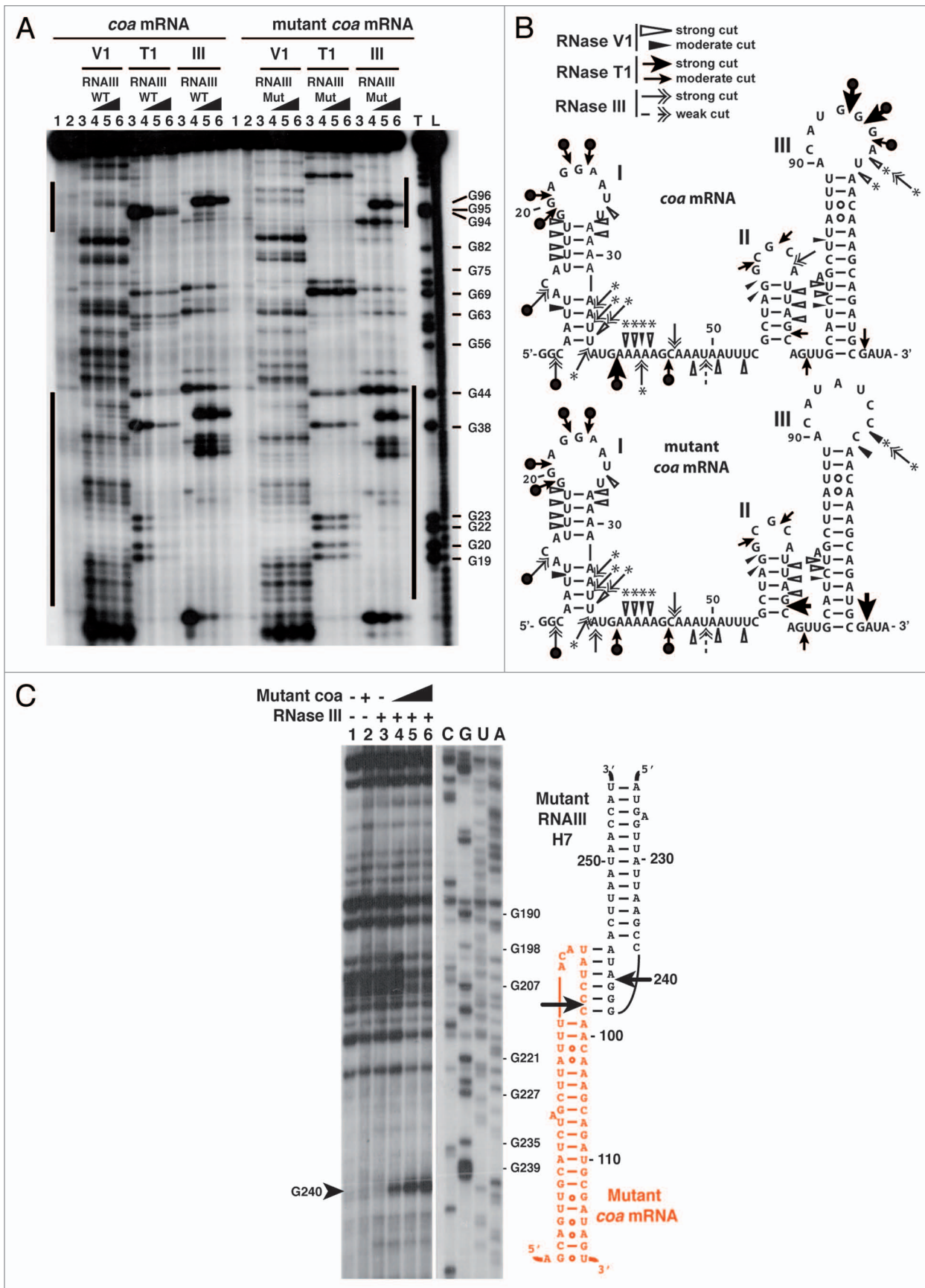


Figure 2. For figure legend, see page 1465.

Figure 2 (See previous page). Comparative enzymatic probing with the WT and mutant RNAIII-*coa* mRNA complexes. (A) Gel fractionation of enzymatic cleavages of 5'-end-labeled wild-type (WT) and mutant *coa* mRNAs. Lanes 1, 2: Incubation controls of mRNA free or bound to RNAIII, respectively; lane 3: RNase hydrolysis on free WT or mutant *coa* mRNAs; lanes 4–6: RNase hydrolysis on WT or mutant *coa* mRNA in the presence of increasing concentrations of WT or mutant RNAIII (lane 4, 50 nM; lane 5, 100 nM; lane 6, 300 nM), respectively; lanes T, L: RNase T1 under denaturing conditions and alkaline ladders, respectively. T1, V1, III: RNase T1, RNase V1 and RNase III hydrolysis, respectively. (B) Enzymatic cleavages are reported on the schematic representation of the secondary structures of WT and mutant *coa* mRNAs. Effect of RNAIII binding: black and white circles are for strong and moderate protection, respectively; stars are for enhancement and new RNase III cuts. (C) RNase III cleavage sites were mapped on in vitro transcribed mutant RNAIII using primer extension with a 5' end-labeled oligonucleotide (see Material and Methods). Lanes 1, 2: Incubation controls of mutant RNAIII free or bound to mutant *coa* mRNA, respectively; lane 3: RNase hydrolysis on free mutant RNAIII; lanes 4–6: RNase hydrolysis on RNAIII in the presence of increasing concentrations of mutant *coa* mRNA (lane 4, 50 nM; lane 5, 100 nM; lane 6, 300 nM). The cleavage sites (arrows) are shown on the secondary structure model of the loop-loop interactions involving the mutated hairpin loop 7 of RNAIII (black) and the mutated hairpin loop III of *coa* mRNA (orange).

G94–G96 in the apical loop III of WT *coa* mRNA toward RNase T1 because of the kissing interaction.

We then compared the RNase III-dependent cleavages using 5'-end labeled WT or mutant mRNAs. The reactions were performed on the free mRNAs as well as on the native WT and mutant RNAIII-*coa* mRNA complexes using a purified His-tagged RNase III from *S. aureus* (Fig. 2A). When the 5' end-labeled mutant mRNA was incubated with mutant RNAIII, four major cleavages occurred at positions 32, 34, 41 and 97 in the mRNA as observed for the WT complex (Figs. 1A and 2A). These cleavages were specific because the addition of Ca²⁺ instead of Mg²⁺ in the buffer inactivated RNase III activity (result not shown). Previous experiments have shown that the hairpin 7 of RNAIII was responsible for the specific RNase III-cleavage at

position 97 of *coa* mRNA while the hairpin 13 of RNAIII promoted major cleavages at positions 32, 34 and 41 in the RBS of *coa* mRNA²⁴ (Fig. 1A). We have also monitored the RNase III cleavage sites in RNAIII using primer extension (Fig. 2C). The data show that binding of the mutant *coa* mRNA to mutant RNAIII induced a major cleavage at G240 in the hairpin loop 7 of RNAIII (Fig. 2C).

In summary, mutations in the sequences of the complementary hairpin loops of RNAIII and *coa* mRNA involved in the kissing interactions do not affect the structure of the mRNA-RNAIII complex nor the recognition by RNase III.

***S. aureus* RNase III cleaves regular RNA-RNA helices and RNA hairpins in a similar manner.** We then analyzed the RNase III-dependent cleavages of regular RNA helices of 30 and

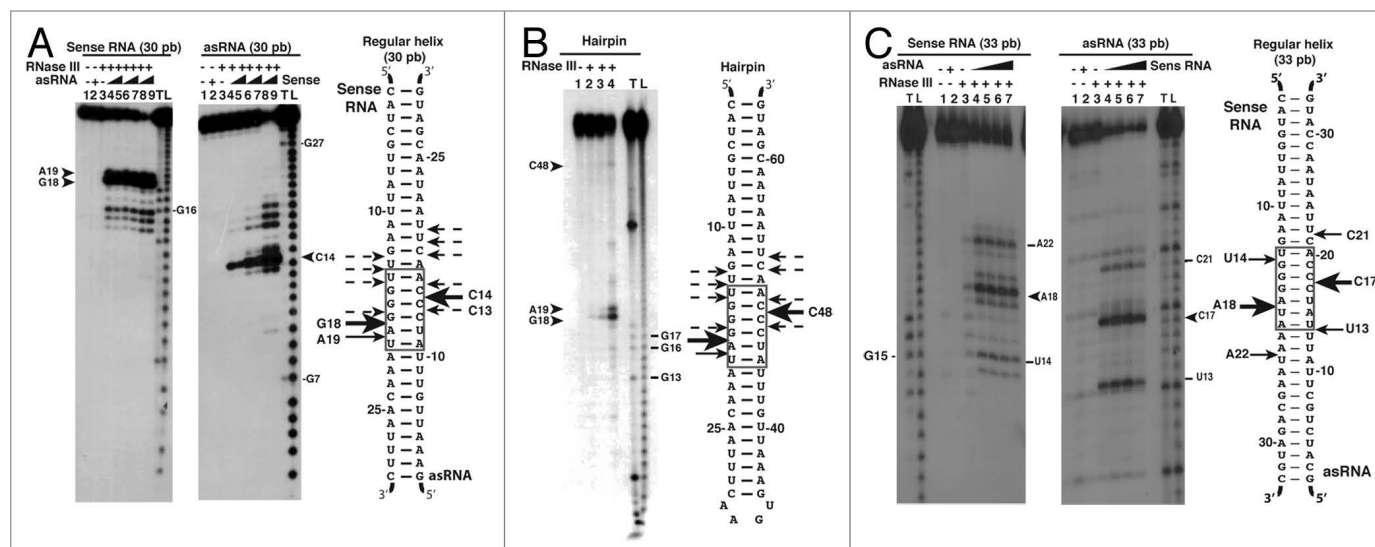


Figure 3. RNase III cleavage assays with various RNA helices. (A) RNase III assays with the 30 bp regular helix. Gel fractionation of RNase III cleavages of 5' end labeled sense RNA strand or antisense RNA (asRNA) strand. Duplex formation was done as described in Material and Methods. Lanes 1, 2: Incubation controls of the 5' end labeled RNA free or in duplex, respectively; lane 3: RNase III (3 μ M) hydrolysis on the 5' end labeled RNA alone; lanes 4–9: RNase III assays performed on the RNA duplex in the presence of increasing concentrations of the complementary strand (lanes 4, 6, 8: 100 nM; lanes 5, 7, 9: 250 nM) and with various concentrations of RNase III (lanes 4, 5: 0.5 μ M; lanes 6, 7: 1 μ M; lanes 8, 9: 3 μ M); lanes T, L: RNase T1 under denaturing conditions and alkaline ladders, respectively. Main RNase III cleavage sites are shown by arrows on one side of the autoradiography. The RNase III cleavages are reported on the RNA secondary structure of the 30 bp helix. Thick, thin and dashed arrows are for strong, moderate and weak cleavages, respectively. The sense and antisense (asRNA) RNA strands are specified. (B) RNase III assays on the 30 bp helix terminated by a tetraloop. Lane 1: Incubation control of the 5' end labeled RNA free; lanes 2–4: RNase III hydrolysis on the 5' end labeled RNA using increasing concentrations of RNase III (lane 2: 0.5 μ M; lane 3: 1 μ M; lane 4: 3 μ M); lanes T, L: RNase T1 under denaturing conditions and alkaline ladders, respectively. The RNase III cleavages are reported on the RNA secondary structure, same legend as above. (C) RNase III assays with the 33 bp regular helix. Lanes 1, 2: Incubation controls of the 5' end labeled RNA free or in duplex, respectively; lane 3: RNase III (1 μ M) hydrolysis with the 5' end labeled RNA; lanes 4–7: RNase III hydrolysis (1 μ M) with the RNA duplex in the presence of increasing concentrations of the complementary strand (lane 4: 50 nM; lane 5: 100 nM; lane 6: 200 nM; lane 7: 300 nM). The RNase III cleavages are reported on the RNA secondary structure of the 33 bp helix using the same legend as above.

33 bp with free ends or terminated by an apical loop (Fig. 3). These helices contained the UGGGAU/AUCCCA pairings at an equivalent position to that found in the kissing interaction of the *coa* mRNA-RNAlIIII complex (Fig. 1A). The RNAs have been chemically synthesized and purified on a denaturing polyacrylamide gel. Prior to RNase III probing, we verified by gel retardation assays that the conditions of hybridization between the two complementary RNAs led to efficient duplex formation at a stoichiometry of 1:1 (result not shown). Either of the two RNA fragments was then labeled at the 5' end and the RNase III cleavage reactions were performed after annealing of the two complementary RNAs, the labeled and the unlabeled strands (Fig. 3A and 3C). The same RNase III reaction was performed on a 5' end-labeled RNA hairpin structure (Fig. 3B).

Within the 30 bp RNA duplex, two strong RNase III-dependent cleavages were mapped at G18 and A19 of the sense RNA strand, and at C13 and C14 of the asRNA strand, leading to two nucleotides 3'-overhang (Fig. 3A). Several additional weak but typical RNase III cleavages were located at G13/U14/U15 on the sense RNA strand and at A17/C18/U19 on the asRNA strand, particularly at high RNase III concentrations (Fig. 3A). These cleavages were specific of the duplex formation because they were not observed in the RNA strands alone (Fig. 3A, lane 3). The same cleavages were found in the hairpin structure, namely at G18, A19, C47 and C48, revealing that the apical loop did not alter the recognition of the RNA by the enzyme. Interestingly, the RNase III cleavages located at A19/C13 in the RNA-RNA duplex and at A19/C47 in the RNA hairpin corresponded to the RNase III cleavages found in the loop-loop interaction. We also analyzed the cleavage pattern on an RNA duplex containing 33 bp. Three main cleavages were obtained at positions U14, A18 and A22 of the sense RNA strand and at positions U13, C17 and C21 of the asRNA strand (Fig. 3C). The strongest cleavages (A18/C17) are located in the middle of the helix while the other cleavages (U14/C21, A22/U13) occurred 12 and 11 bp from the 3' end. Thus, the cleavage pattern of the 33 bp helix is somehow different to that obtained for the 30 bp helix although the main cleavages at A18/C17 take place in the other constructs (Fig. 3).

Taken together these data showed that the RNA helix structure, i.e., number of base pairs, rather than the sequence direct the RNase III cleavages. In addition, an apical loop does not affect the RNase III cleavage location in the regular helix. In contrast to the loop-loop complex, the regular helices are cleaved at several positions leading to 11 bp fragments.

A bulged loop restrained the number of RNase III cleavages in the helix. In order to create an irregularity into the regular 30 bp helix, we have introduced a bulged loop 5' to the UGGGAU/AUCCCA base pairings (Fig. 4). The RNAs were chemically synthesized and purified on a denaturing polyacrylamide gel and the conditions of hybridization between two complementary RNA strands were optimized (results not shown). After 5' end labeling, the RNase III cleavage reactions were performed on the free RNAs and the pre-formed RNA duplexes (Fig. 4A and 4B). The data revealed that only one strong cleavage occurred at C13 of the asRNA strand and at A23 of the sense RNA strand when the RNA duplex was formed (Fig. 4A and 4C). Hence, the

addition of the bulged loop restrained the number of RNase III binding sites in comparison to the 30 bp regular helix (Fig. 4C).

The same experiment was performed with the 36 bp helix interrupted by the same internal loop (Fig. 4B). Two major RNase III cleavages were found at A29 and A30 of the sense RNA strand and at U13 and A14 of the asRNA strand, giving a two nucleotides 3'-overhang (Fig. 4C). Other weaker but typical RNase III cleavages were also detected (Fig. 4B). The RNase III cleavage patterns obtained with the interrupted 29 bp and 36 bp helices are very different. Thus, increasing the number of consecutive Watson-Crick (WC) base pairings created other preferred RNase III binding sites centered in the helix.

RNase III does not improve the repressor activity of RNAlIIII on *coa* mRNA translation. Knowing that RNase III contributed to the efficiency of the RNAlIIII-dependent repression of *coa* mRNA,²⁴ we monitored whether the enzyme is able to stabilize the binding of RNAlIIII to *coa* mRNA and/or to contribute to the efficiency of translation repression. Recent biochemical analysis performed on *S. aureus* RNase III showed that the two conserved acidic residues, E135 and D63, are essential for catalysis, as their substitution by alanine compromised cleavages without affecting RNA binding.¹⁶ These acidic residues are part of the catalytic site, which together with two Mg²⁺ ions perform the stepwise hydrolysis of the phosphodiester bonds.²⁹ The catalytically inactive E135A variant of RNase III carrying a histidine epitope tag at its N-terminus was purified to homogeneity following expression in *E. coli*.^{16,21} We first used gel retardation assays to monitor the effect of E135A mutant enzyme on complex formation between terminally labeled *coa* mRNA and RNAlIIII. The data showed that the mutant E135A enzyme was able to bind the mRNA-RNAlIIII complex but had no significant effect on the duplex stability (results not shown).

We then analyzed whether the binding of RNase III E135A to the mRNA-RNAlIIII complex contributes to the occlusion of the ribosome recruitment to its loading site. Toeprinting assays were performed to monitor the formation of the ternary complex between the *S. aureus* 30S subunits, *coa* mRNA and the initiator tRNA^{Met}. A 5' end-labeled primer was first annealed to *coa* mRNA, followed by the addition of increasing concentrations of RNase III E135A in the presence of RNAlIIII, the 30S subunits and the tRNA. The experiment revealed that RNAlIIII binding alone was sufficient to prevent efficiently the ribosome binding. However, we have observed the appearance of a reverse transcriptase stop at position G+3 as the result of the interaction between RNAlIIII and RNase III E135A (Fig. 5, lane 4). Because RNase III E135A has lost its catalytic activity,¹⁶ these data suggest that RNase III binding to the RNAlIIII-*coa* mRNA regulatory complex arrest reverse transcriptase elongation.

Discussion

Studies in *E. coli* revealed that the RNase III enzyme cleaves regular helices with little sequence specificity.^{26,30,31} These data showed that several RNA substrates contained both positive and negative determinants allowing RNase III to cleave at a precise and specific position of a model RNA hairpin.^{26,27} Extensive

mutations performed on this RNA hairpin demonstrated that the RNA sequence extending 10–11 base pairs from the cleavage site affected the RNase III activity.^{26,27} These studies revealed two main regions in the RNA helix that mostly contributed to the enzyme recognition, i.e., the proximal box comprising the first 4 bp adjacent to the cleavage site and the distal box located 8 bp after the cut. Interestingly, the proximal box contains both positive and negative determinants, which cooperate to define the cleavage efficiency and specificity.^{26,27} The crystal structure of *Aquifex aeolicus* RNase III in complex with different dsRNAs^{29,31} identified a large RNA-binding surface cleft called the catalytic valley, which accommodates the dsRNA. The contacts between protein and RNA span almost 11 bp from the cleavage site, and the hydrolysis of each strand requires the two subunits.^{26,29,31,32} Furthermore, the dsRNA and the protein undergo significant conformational changes during catalysis mediated through two Mg²⁺ ions.²⁹ Each subunit of the protein contains four RNA binding motifs (RBM) where RBM1, RBM2 and RBM4 interact with the proximal, middle and distal sites of the helix, respectively, and RBM3 binds closely to the cleavage site (Fig. 6A). Emerging

from these studies, a model was proposed where the RNA substrate is first selected by RBM1 and RBM2 and then transferred to the catalytic site for scissile bond selection, mainly through RBM3.^{26,29,31,32} All these important findings provided some rules explaining how bacterial RNase III selects RNA substrates for binding and cleavage.

Besides regular helices, the *E. coli* enzyme was shown to bind and cleave a variety of structures such as coaxially stacked short helices³³ or dsRNA interrupted by internal loops.^{16,34} We show here that *S. aureus* RNase III cleaves loop-loop interactions at a specific site, which is not strictly dependent on the nature of the WC base pairs (Figs. 1 and 6). The base pair substitutions introduced at the kissing interactions formed between *coa* mRNA and the quorum sensing regulatory RNAIII had no significant effect on the cleavage reaction and specificity. Therefore, we propose that the loop-loop interaction provides a unique local structure to direct the RNase III cleavages at single positions of the kissing interactions. This was visualized on a three-dimensional model of the kissing interactions, which took into account the chemical probing data.²⁴ The model revealed a co-axial stacking of the

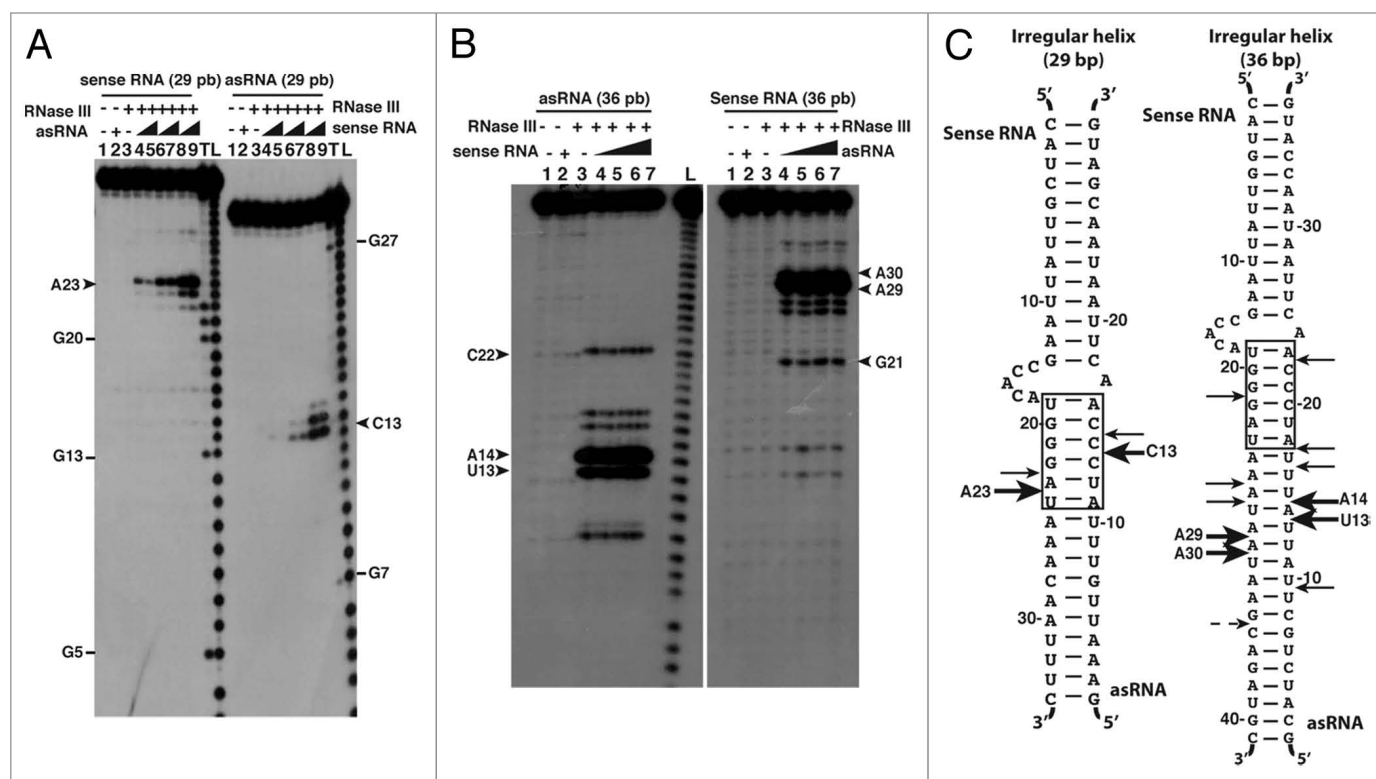


Figure 4. RNase III cleavage assays with the 29 bp and 36 bp regular helices interrupted by an internal loop. (A) Gel fractionation of RNase III cleavages of 5'-end-labeled sense RNA strand or asRNA strand (29 bp irregular helix). Duplex formation was done as described in Material and Methods. Lanes 1, 2: Incubation controls of the 5' end labeled RNA free or in duplex, respectively; lane 3: RNase III hydrolysis (1 μM) on the 5' end labeled RNA; lanes 4–9: RNase III hydrolysis on the RNA duplex in the presence of increasing concentrations of the complementary strand (lanes 4, 6, 8: 100 nM; lanes 5, 7, 9: 250 nM) with various concentrations of RNase III (lanes 4, 5: 0.5 μM; lanes 6, 7: 1 μM; lanes 8, 9: 3 μM); lanes T, L: RNase T1 under denaturing conditions and alkaline ladders, respectively. (B) Gel fractionation of RNase III cleavages of 5'-end-labeled sense RNA strand or antisense RNA (asRNA) strand (36 bp irregular helix). Lanes 1, 2: Incubation controls of 5' end labeled RNA free or in duplex, respectively; lane 3: RNase III hydrolysis (1.5 μM) on free 5' end labeled RNA; lanes 4–7: RNase III hydrolysis (1.5 μM) was performed on the RNA duplex in the presence of increasing concentrations of one of the complementary strand (lane 4: 50 nM; lane 5: 100 nM; lane 6: 200 nM; lane 7: 300 nM); lane L: alkaline ladder. (C) The RNase III cleavages are reported on the 29 and 36 bp helices interrupted by an internal loop. Thick, thin and dashed arrows are for strong, moderate and weak cleavages, respectively. The sense and antisense strands are specified. The sequences corresponding to the kissing interactions as found in RNAIII-*coa* mRNA complex are boxed.

intermolecular and intramolecular helices to form a long helical structure harboring a slight bent (Fig. 6A). This RNA structure model was then docked into the crystal structure of the dsRNA-bound form of *Aquifex* RNase III.³¹ It shows that the loop-loop interaction almost perfectly fitted into the catalytic valley with the two cleavage sites located on the same face close to the Mg²⁺ ion and the conserved acidic residues (Fig. 6B).

Using the catalytically-defective mutant RNase III E135A,¹⁶ we showed that the mutant enzyme did not improve either the binding of *S. aureus* RNAIII to *coa* mRNA nor the capacity of RNAIII to prevent the formation of the initiation complex (Fig. 5). These in vitro data support the hypothesis that *S. aureus* RNase III is required to irreversibly arrest the synthesis of coagulase by initiating the degradation of the repressed mRNA.²³ The loop-loop interaction provides an ideal RNase III binding site to initiate the degradation of structured elements in the mRNA. *S. aureus* RNAIII and RNase III were also shown to conjointly repress the translation of *rot* mRNA.^{22,23} In this system, two stem-loop structures of the regulatory RNA base pair to two complementary hairpin loops within the 5'UTR of *rot* mRNA. A single loop-loop interaction is not sufficient for repression and both kissing interactions contribute to regulation: one contact occludes the RBS while the second one stabilizes the duplex.²³ In addition, *rot* mRNA was processed by RNase III in vivo when RNAIII was produced.²³ The sequences of the two loop-loop interactions between *S. aureus* RNAIII and *rot* mRNA are almost identical to that found in RNAIII-*coa* mRNA^{22,23} (Fig. 1A). While the two loops of *rot* mRNA were cleaved by RNase III similarly to *coa* mRNA, only the loop of RNAIII which was bound to the SD of *rot* mRNA was efficiently cleaved²³ (Fig. 1). What could be the molecular explanation for the different behavior of RNase III on the two kissing interactions? The crystal structure of *Aquifex* RNase III showed that the double-stranded RNA binding domains (dsRBDs) are connected to the ribonuclease domains by flexible linkers.³² In the structure of the protein bound to an RNA-RNA duplex, the RBM1 and RBM2 interact on the opposite side of the RNA helix making contacts with the sugar-phosphate backbone of the minor groove.^{29,31} The three-dimensional model of the kissing interaction sequestering the SD sequence of *rot* mRNA was built and docked on the crystal structure of the dsRNA-bound form of *Aquifex* RNase III (Fig. 6C). The model shows that the large connecting loop crossing the deep major groove of the kissing interactions makes a steric clash with RBM1 of one monomer (Fig. 6C). Interestingly, it was proposed that RBM1, which binds 1 bp from the scissile bond, should contribute to the organization of the catalytic site structure.²⁹ Therefore, we suggest that the large connecting loop acts as a steric anti-determinant for catalysis by altering the positioning of RBM1 and RBM2. Because several small asRNAs and their target RNAs initiate fast binding by defined loop-loop contacts, they create potential substrates for RNase III.^{35,36} One characteristic example is *E. coli* OxyS sRNA, which represses translation of *flhA* mRNA through base-pairings between two non-contiguous regions involving loop-loop interactions.³⁷ The sequence of one of the kissing interactions (AGGGUU/AACCCU), which sequestered the SD sequence of *flhA*, is very similar to the base pairings

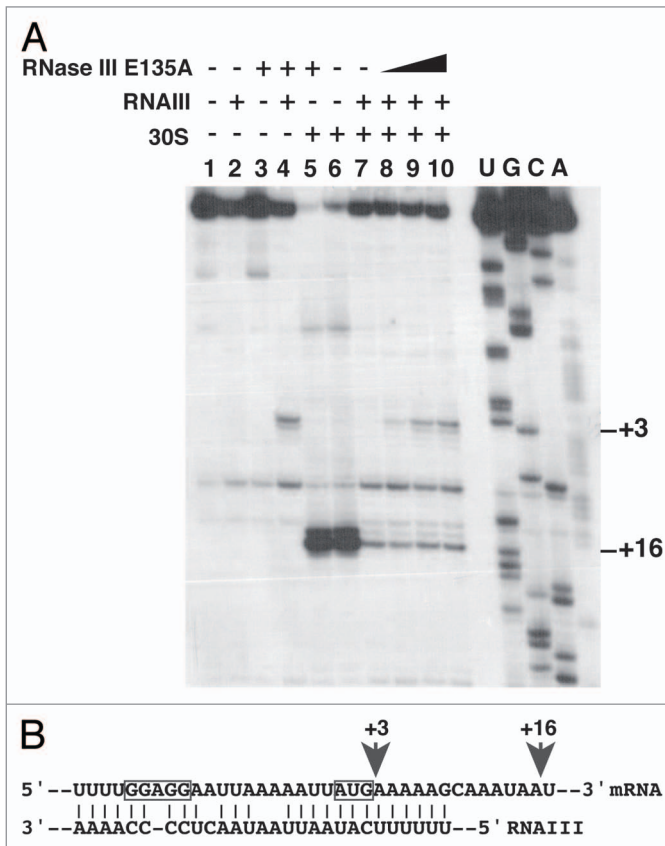


Figure 5. Effect of the catalytically-inactive RNase III E135A mutant on ribosome binding with *coa* mRNA. **(A)** Toeprinting assays. Formation of the ternary complex between *coa* mRNA (15 nM), *S. aureus* 30S ribosomal subunits (250 nM) and initiator tRNA (1 μM) was monitored in the absence (lane 5, 6) and in the presence of wild-type RNAIII (lanes 7–10: 100 nM). Various concentrations of RNase III E135A mutant are also added (lane 8: 0.5 μM; lane 9: 1 μM; lane 10: 3 μM). The toeprint at position +16 is indicated. Incubation controls with free RNA are shown in lane 1, in the presence of RNAIII in lanes 2 and 4 and with RNase III E135A in lanes 3 and 4. Lanes U, G, C, A correspond to dideoxy-sequencing reactions performed with *coa* mRNA. **(B)** RNAIII binds to the ribosome binding site of *coa* mRNA. Arrows denote the reverse transcriptase pauses: the pause at position +3 was induced by the simultaneous binding of RNAIII and RNase III E135A to *coa* mRNA while the pause at position +16 corresponded to the 30S-tRNA-mRNA complex formation (toeprint).

found in *coa*-RNAIII and *rot*-RNAIII complexes suggesting that OxyS-*flhA* mRNA complex might represent another novel target for *E. coli* RNase III cleavage.

To analyze the influence of the UGGGAU/AUCCCA interaction on RNase III recognition and cleavage, this module has been introduced into regular helices of different sizes, in helices interrupted by bulged loops, and in a stem-loop structure (Fig. 1). As described above, the homodimeric RNase III enzyme covers 22 bp of RNA-RNA duplex leading to cleavage staggered by two base pairs after 11 bp on each strand. Statistically, the enzyme can bind at several positions but will cleave only if the helical length requirements are satisfied. With this ruler, all cleavages obtained on the different helices and hairpins can be readily explained. For instance, two major and several weak RNase III cleavage sites on

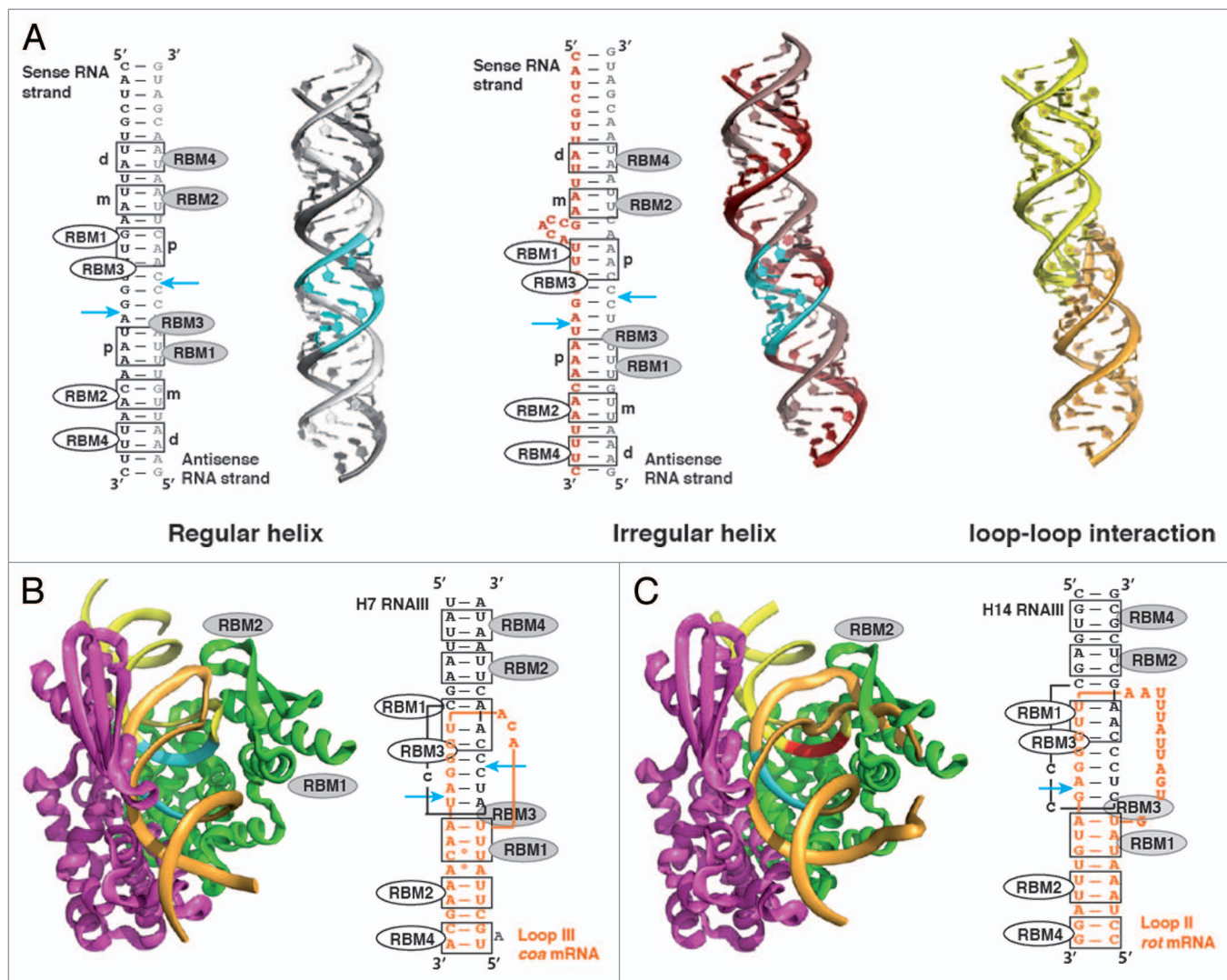


Figure 6. Three-dimensional models of various RNA-RNA duplexes and interaction with RNase III. **(A)** Models represented the regular 30 bp helix (in gray), the 29 bp helix interrupted by a bulged loop (in red) and the kissing interactions as found in RNAIII (yellow)-*coa* mRNA (orange). The III-D representations were drawn with PYMOL program. The schematic views of the RNA duplexes (30 bp regular helix, 29 bp interrupted helix) with the positioning of the RNA binding domains (RBM) of RNase III are based on the crystal structure of *Aquifex aeolicus* RNase III bound to dsRNA:^{29,31} the boxed nucleotides represent the proximal (p), middle (m) and distal (d) boxes from the major cleavage sites that are recognized by RBM1 to RBM4 of RNase III. The RBMs for each RNase III subunit are represented by different colors. **(B,C)** Docking of the kissing complexes of *coa* mRNA-RNAIII **(B)** and of *rot* mRNA-RNAIII **(C)** on the crystal structure of *Aquifex aeolicus* RNase III containing Mg^{2+} (from ref. 29; pdb coordinates 2NUG). The two subunits of RNase III are colored in magenta and green. The hairpin loop of RNAIII is colored in yellow and the mRNA in orange. The cleavage sites are in blue. The site that is not cleaved by RNase III in *rot*-RNAIII kissing interaction is in red. A steric clash is visualized between the connecting loop of the kissing interactions and one of the double stranded RNA binding domain (dsRBD) domain of RNase III. Schematic views represented the kissing interactions as it is found in **(B)** *coa* mRNA-RNAIII and **(C)** *rot*-RNAIII duplexes. Same legend as in **Figure 6A**. Nucleotides of the hairpin H7 of RNAIII are colored in black and nucleotides of the mRNA hairpin are in orange.

each strand were found in the 30 bp long RNA duplex, leading to RNA fragments of 10–11 bp. However, the major cleavages were obtained within the G-C rich sequence motif indicating that the stacking of nucleotides might locally favor the binding of RNase III. Closing the 30 bp helix with a tetraloop did not modify the reactivity of the enzyme and the cleavage positions were identical to the parental helix. This indicated that the presence of an apical loop did not determine the cleavage site selection as it was shown for the homologous yeast enzyme where the cut is determined by the distance from a tetraloop motif.³⁸ In

contrast, the introduction of an asymmetrical internal loop in the middle of the 30 bp helix did not create a new cleavage site but restrained the number of *S. aureus* RNase III cuts (Fig. 4). Structure modeling suggested that the bulged loop behaves as a negative signature and prevents the RNase III recognition of the upper helix due to steric hindrance. The addition of 3 bp to the 30 bp regular helix or 6 bp to the interrupted helix drastically changed the RNase III cleavage patterns (Figs. 3 and 4). In both cases, typical and strong RNase III cleavages occurred on both strands located at the middle of the helix. Recent studies based

on co-immunoprecipitation assays and deep sequencing identified novel RNA substrates of *S. aureus* RNase III.¹⁶ Several of the RNAs are characterized by hairpin loops that are cleaved on both sides of 22–25 bp long helices at unique positions leading to RNA fragments of 9 to 12 bp with 2 nt 3'-overhang (Fig. S1). We did not observe any particular sequence motifs although the stems are A-U/U-A rich and carry several non-canonical base pairs.

RNA loop-loop interactions are adapted structural motifs that contribute to specific molecular recognition not only because of WC complementarity between the paired regions but also because the fold topology imposes additional constraints.^{35,36} This study shows that loop-loop interactions connected by short unpaired regions formed by the binding of a regulatory RNA to its target mRNAs represent a unique topology that creates a single binding site for *S. aureus* RNase III. With a small number of intermolecular base pairs, it is possible to reconstitute an RNase III binding site by forming coaxially stacked short helices. Thus, the topology of sRNA-mRNA complex is an important aspect of RNase III recognition and cleavage. Depending on the mRNA binding site, loop-loop interactions are also expected to enhance the decay rate of mRNA independently of translation repression, or to induce specific mRNA maturation leading to stabilization. In addition, we showed that the sequence of the helix, the number of consecutive WC including non-canonical base pairs, and the presence of bulged nucleotides contribute in a positive or negative manner to induce or prevent RNase III cleavages, respectively. We anticipate that careful analysis of the whole set of RNA substrates of *S. aureus* RNase III should unravel unexpected RNA topologies recognized by the enzyme that might play important roles in RNA decay, processing or gene regulation.

Methods and Materials

RNA preparation. RNAIII, fragments of *coa* mRNA (including the whole 5'UTR and 126 nt of the coding sequence), and *rot* mRNA (including the whole 5'UTR and 100 nt of the coding sequence) were transcribed in vitro using home-made T7 RNA polymerase.³⁹ Mutations have been introduced in the hairpin loop 7 of RNAIII (AUCCCA245 changed by GGGUAU245) and in the coding region of *coa* mRNA (UGGGAU98 changed by UAUCCC98) using the Quickchange XL Site-directed mutagenesis protocol (Stratagene). The oligonucleotides used for the mutagenesis of *coa* mRNA were AGC AGT TGC ATC TAG CTT ATT TAC ATA TCC CAA CAA AGC AGA TGC GTA GT and its antisense, and for RNAIII, CTA AAG TAT GAG TTA TTA AGC CGG GAT AAC TTA ATA ACC ATG TAA AAT T and its antisense; nucleotides in italic represented the mutation sites. The transcribed RNAs were purified by 8% polyacrylamide-8 M urea gel electrophoresis. After elution in 0.5 M ammonium acetate/1 mM EDTA buffer, the RNAs were precipitated twice with ethanol. Before use, the pellets were dissolved in sterile bi-distilled water and the concentration was measured accurately. The various RNA fragments were chemically synthesized by Integrated DNA Technologies (Belgium). The RNAs were purified on HPLC and their quality was verified on a 15% polyacrylamide-8 M urea gel electrophoresis.

The 5' end-labeling of dephosphorylated transcribed RNA or of the chemically synthesized RNA was performed with T4 polynucleotide kinase and [γ -³²P]ATP. Before use, RNAs were renatured by incubation at 90°C for 2 min in water, 1 min on ice, followed by an incubation step at 20°C for 15 min in TMN buffer (20 mM TRIS-acetate pH 7.5, 10 mM magnesium-acetate, 150 mM Na-acetate).

Complex formation between sense RNA and asRNA strands was formed under denaturing and native conditions. The 5' end-labeled or unlabeled RNA (3 $\times 10^{-8}$ M) was mixed with a 5-fold excess of unlabeled complementary RNA and duplexes were formed by incubation of the two RNAs at 90°C for 2 min followed by slow cooling to 37°C in TMN buffer. Duplex formation was monitored on gel retardation assays using 8% PAGE under non-denaturing conditions.

RNase III purification. Wild-type and mutant RNase III E135A were cloned in vectors pQE30 derivatives and the plasmids were transformed into *E. coli* strain M15[pREP4]. Overexpression and purification of the two enzymes carrying 6 histidines at their N-terminus were done as described previously.¹⁶ After cell growth and grinding, the soluble fraction of the protein was precipitated by gentle addition of 4.58 g of ammonium sulfate (2 M final concentration) for 1 h on ice, and centrifuged (30 min, 10,000 rpm, 4°C). The pellet was dissolved in 10 ml of 25 mM TRIS-HCl (pH 8.0), 0.1 mM EDTA, and was incubated with the Ni²⁺-beads (Qiagen) for 1 h at 4°C. After successive washing steps, the enzymes were eluted using 500 mM of imidazole in 25 mM of TRIS-HCl (pH 8), 1 M NH₄Cl, 1 mM DTT. The fractions containing the protein were then directly loaded on a polyI-polyC chromatography (Pharmacia) pre-equilibrated with 25 mM of TRIS-HCl (pH 8), 1 M NH₄Cl, 1 mM DTT and the elution is done in the same buffer containing 2 M NH₄Cl. The purified WT and RNase III E135A were then dialyzed at 4°C against 30 mM TRIS-HCl pH 8.0, 500 mM KCl, 0.1 mM DTT, 0.1 mM EDTA, 50% bidistilled glycerol. Mass spectrometry analysis was performed on the purified enzyme.

RNase III cleavage assays. The RNase III cleavage assay was done either on 5' end-labeled (50000 cpm) or unlabeled RNA (1–2 pmol). Reaction was performed with purified RNase III (0.5–2 μ M), 1 μ g of yeast total tRNA in 10 mM TRIS-HCl, pH 8, 10 mM MgCl₂, 100 mM KCl, DTT 1 mM for 5 min at 37°C.

Primer extension was used to assign the RNase III cleavages on unlabeled RNA. The cleaved RNA was hybridized with a 5'-labeled oligonucleotide complementary to the hairpin loop of H7 of RNAIII (0.4 pmol; ATT ATC TGT AAT GAT AAT TAA GAA) as follows: 90°C for 1 min, 1 min on ice and then incubated at 20°C for 15 min in 50 mM TRIS-HCl pH 7.5, 20 mM MgCl₂, 50 mM KCl. Reverse transcription was performed with 0.3 mM dNTPs and 0.1 U/ μ l RT (AMV) at 37°C for 30 min. After destruction of the RNA template, samples were run on 8% polyacrylamide-7 M urea gels. Sequencing reactions were done in parallel on the RNA transcripts. When 5' end-labeled RNA was used, the cleavages were assigned using RNase T1 hydrolysis performed under denaturing conditions and an alkaline ladder.

Enzymatic structure probing. The secondary structure of 5' end-labeled WT or mutant *coa* mRNA free (1–2 pmol) or bound

to WT or mutant RNAIII (50–250 nM) was probed by RNase T1 and RNase V1. Complex formation was performed on previously renatured RNAs at 37°C for 15 min in 10 µl of buffer containing 10 mM TRIS-HCl, pH 8, 10 mM MgCl₂, 100 mM KCl, 1 mM DTT. Enzymatic hydrolysis were performed at 37°C for 5 min in the presence of 1 µg carrier tRNA with RNase T1 (0.0025 U) or RNase V1 (0.1 U). Reactions were stopped by phenol/chloroform extraction followed by ethanol precipitation. Incubation controls were done in parallel to detect nicks in the RNA and the cleavages were assigned using RNase T1 hydrolysis under denaturing conditions and an alkaline ladder.

Toeprinting assays. The formation of a simplified translational initiation complex with *coa* mRNA was done using published procedure.⁴⁰ *Coa* mRNA was annealed to the 5' end-labeled oligonucleotide (complementary to nucleotides 99 to 117) in 20 mM TRIS-acetate pH 7.5, 60 mM NH₄Cl, 3 mM β-mercaptoethanol, heated at 90°C for 1 min and cooled on ice for 1 min. Mg-acetate was added at 10 mM final concentration and incubation was continued at 20°C for 20 min. Initiation complex formation was performed at 37°C for 15 min in 10 mM TRIS-acetate pH 7.4, 60 mM NH₄Cl, 10 mM Mg-acetate, 6 mM β-mercaptoethanol in the presence of *coa* mRNA annealed to the labeled primer, 0.1–0.5 µM 30S subunits and 1 µM initiator tRNA^{fMet}. Primer extension reactions were subsequently performed by adding 2–4 units of AMV reverse transcriptase at 37°C for 15 min. Reactions were stopped by phenol extraction followed by ethanol precipitation, and samples were loaded on 8% polyacrylamide-8 M urea slab gels.

Molecular modeling. Modeling of the kissing interactions of the *coa* mRNA (residues U73 to A114) with the hairpin loop 7 of RNAIII (residues A223 to U256), of the hairpin loop containing the SD sequence of *rot* mRNA (residues G205 to C240) bound to the hairpin loop 14 of RNAIII (residues G484 to C512), of a

30 bp regular helix, and of a 30 bp helix interrupted by a bulged loop were performed as previously described.^{41,42} After the interactive assembly step, several cycles of geometrical least-square refinements were performed until a satisfactory solution was reached. The III-D models of the kissing interactions were docked on the crystal structure of *Aquifex aeolicus* RNase III containing Mg²⁺. The pdb coordinates (2NUG) corresponded to the active form of the protein complexed to a cleaved dsRNA.²⁹ The pictures were prepared using the PYMOL program (DeLano WL, The PyMOL Molecular Graphics System 2002; www.pymol.org).

Disclosure of Potential Conflicts of Interest

No potential conflicts of interest were disclosed.

Acknowledgments

We are thankful to E. Lioliou, I. Caldelari, P. Fechter, C. Condon and S. Boisset for helpful discussions and careful reading of the manuscript. We are grateful to E. Lioliou who has prepared the RNase III E135A mutant, and Anne-Catherine Helfer for technical help. This work was supported by the Centre National de la Recherche Scientifique (CNRS, P.R.), Université de Strasbourg (UdS, E.W.), the Institut National pour la Recherche Médicale (INSERM, F.V. and T.G.), the Agence Nationale pour la Recherche (ANR: ANR09-BLAN-0024–01; ANR10-Pathogenomics-ARMSA; P.R. and F.V.), and the “Laboratoires d’Excellence” (LABEX) NetRNA Grant (ANR-10-LABX-36, E.W. and P.R.). CR was supported by fellowships from Délégation Générale de l’Armement (DGA), Région Alsace, and the Fondation pour la Recherche Médicale.

Supplemental Materials

Supplemental materials may be found here: www.landesbioscience.com/journals/rnabiology/article/22710

References

- Dinges MM, Orwin PM, Schlievert PM. Exotoxins of *Staphylococcus aureus*. Clin Microbiol Rev 2000; 13:16-34; PMID:10627489; <http://dx.doi.org/10.1128/CMR.13.1.16-34.2000>.
- Foster TJ, Höök M. Surface protein adhesins of *Staphylococcus aureus*. Trends Microbiol 1998; 6:484-8; PMID:10036727; [http://dx.doi.org/10.1016/S0966-842X\(98\)01400-0](http://dx.doi.org/10.1016/S0966-842X(98)01400-0).
- Novick RP. Autoinduction and signal transduction in the regulation of staphylococcal virulence. Mol Microbiol 2003; 48:1429-49; PMID:12791129; <http://dx.doi.org/10.1046/j.1365-2958.2003.03526.x>.
- Novick RP, Geisinger E. Quorum sensing in staphylococci. Annu Rev Genet 2008; 42:541-64; PMID:18713030; <http://dx.doi.org/10.1146/annurev.genet.42.110807.091640>.
- Anderson KL, Dunman PM. Messenger RNA Turnover Processes in *Escherichia coli*, *Bacillus subtilis*, and Emerging Studies in *Staphylococcus aureus*. Int J Microbiol 2009; 2009:525491; PMID:19936110; <http://dx.doi.org/10.1155/2009/525491>.
- Anderson KL, Roberts C, Disz T, Vonstein V, Hwang K, Overbeek R, et al. Characterization of the *Staphylococcus aureus* heat shock, cold shock, stringent, and SOS responses and their effects on log-phase mRNA turnover. J Bacteriol 2006; 188:6739-56; PMID:16980476; <http://dx.doi.org/10.1128/JB.00609-06>.
- Anderson KL, Roux CM, Olson MW, Luong TT, Lee CY, Olson R, et al. Characterizing the effects of inorganic acid and alkaline shock on the *Staphylococcus aureus* transcriptome and messenger RNA turnover. FEMS Immunol Med Microbiol 2010; 60:208-50; PMID:21039920; <http://dx.doi.org/10.1111/j.1574-695X.2010.00736.x>.
- Jester BC, Romby P, Lioliou E. When ribonucleases come into play in pathogens: a survey of gram-positive bacteria. Int J Microbiol 2012; 2012:592196; PMID:22550495; <http://dx.doi.org/10.1155/2012/592196>.
- Roux CM, DeMuth JR, Dunman PM. Characterization of components of the *Staphylococcus aureus* mRNA degradosome holoenzyme-like complex. J Bacteriol 2011; 193:5520-6; PMID:21764917; <http://dx.doi.org/10.1128/JB.05485-11>.
- Kaberlin VR, Singh D, Lin-Chao S. Composition and conservation of the mRNA-degrading machinery in bacteria. J Biomed Sci 2011; 18:23-35; PMID:21418661; <http://dx.doi.org/10.1186/1423-0127-18-23>.
- Olson PD, Kuechenmeister LJ, Anderson KL, Daily S, Beenken KE, Roux CM, et al. Small molecule inhibitors of *Staphylococcus aureus* RnpA alter cellular mRNA turnover, exhibit antimicrobial activity, and attenuate pathogenesis. PLoS Pathog 2011; 7:e1001287; PMID:21347352; <http://dx.doi.org/10.1371/journal.ppat.1001287>.
- Marincola G, Schäfer T, Behler J, Bernhardt J, Ohlsen K, Goerke C, et al. RNase Y of *Staphylococcus aureus* and its role in the activation of virulence genes. Mol Microbiol 2012; 85:817-32; PMID:22780584; <http://dx.doi.org/10.1111/j.1365-2958.2012.08144.x>.
- Kaito C, Kurokawa K, Matsumoto Y, Terao Y, Kawabata S, Hamada S, et al. Silkworm pathogenic bacteria infection model for identification of novel virulence genes. Mol Microbiol 2005; 56:934-44; PMID:15853881; <http://dx.doi.org/10.1111/j.1365-2958.2005.04596.x>.
- Liu Y, Dong J, Wu N, Gao Y, Zhang X, Mu C, et al. The production of extracellular proteins is regulated by ribonuclease III via two different pathways in *Staphylococcus aureus*. PLoS One 2011; 6:e20554; PMID:21655230; <http://dx.doi.org/10.1371/journal.pone.0020554>.
- Huntzinger E, Boisset S, Saveanu C, Benito Y, Geissmann T, Namane A, et al. *Staphylococcus aureus* RNAIII and the endoribonuclease III coordinately regulate *spa* gene expression. EMBO J 2005; 24:824-35; PMID:15678100; <http://dx.doi.org/10.1038/sj.emboj.7600572>.
- Lioliou E, Sharma CM, Caldelari I, Helfer AC, Fechter P, Vandenesch F, et al. Global regulatory functions of the *Staphylococcus aureus* endoribonuclease III in gene expression. PLoS Genet 2012; 8:e1002782; PMID:22761586; <http://dx.doi.org/10.1371/journal.pgen.1002782>.

17. MacRae IJ, Doudna JA. Ribonuclease revisited: structural insights into ribonuclease III family enzymes. *Curr Opin Struct Biol* 2007; 17:138-45; PMID:17194582; <http://dx.doi.org/10.1016/j.sbi.2006.12.002>.
18. Conrad C, Schmitt JG, Evgueniev-Hackenberg E, Klug G. One functional subunit is sufficient for catalytic activity and substrate specificity of *Escherichia coli* endoribonuclease III artificial heterodimers. *FEBS Lett* 2002; 518:93-6; PMID:11997024; [http://dx.doi.org/10.1016/S0014-5793\(02\)02653-4](http://dx.doi.org/10.1016/S0014-5793(02)02653-4).
19. Dasgupta S, Fernandez L, Kameyama L, Inada T, Nakamura Y, Pappas A, et al. Genetic uncoupling of the dsRNA-binding and RNA cleavage activities of the *Escherichia coli* endoribonuclease RNase III--the effect of dsRNA binding on gene expression. *Mol Microbiol* 1998; 28:629-40; PMID:9632264; <http://dx.doi.org/10.1046/j.1365-2958.1998.00828.x>.
20. Sun W, Jun E, Nicholson AW. Intrinsic double-stranded-RNA processing activity of *Escherichia coli* ribonuclease III lacking the dsRNA-binding domain. *Biochemistry* 2001; 40:14976-84; PMID:11732918; <http://dx.doi.org/10.1021/bi011570u>.
21. Chevalier C, Huntzinger E, Fechter P, Boisset S, Vandenesch F, Romby P, et al. *Staphylococcus aureus* endoribonuclease III purification and properties. *Methods Enzymol* 2008; 447:309-27; PMID:19161850; [http://dx.doi.org/10.1016/S0076-6879\(08\)02216-7](http://dx.doi.org/10.1016/S0076-6879(08)02216-7).
22. Geisinger E, Adhikari RP, Jin R, Ross HF, Novick RP. Inhibition of rot translation by RNAlII, a key feature of agr function. *Mol Microbiol* 2006; 61:1038-48; PMID:16879652; <http://dx.doi.org/10.1111/j.1365-2958.2006.05292.x>.
23. Boisset S, Geissmann T, Huntzinger E, Fechter P, Bendridi N, Possedko M, et al. *Staphylococcus aureus* RNAlII coordinately represses the synthesis of virulence factors and the transcription regulator Rot by an antisense mechanism. *Genes Dev* 2007; 21:1353-66; PMID:17545468; <http://dx.doi.org/10.1101/gad.423507>.
24. Chevalier C, Boisset S, Romilly C, Masquida B, Fechter P, Geissmann T, et al. *Staphylococcus aureus* RNAlII binds to two distant regions of coa mRNA to arrest translation and promote mRNA degradation. *PLoS Pathog* 2010; 6:e1000809; PMID:20300607; <http://dx.doi.org/10.1371/journal.ppat.1000809>.
25. Lasa I, Toledo-Arana A, Dobin A, Villanueva M, de los Mozos IR, Vergara-Irigaray M, et al. Genome-wide antisense transcription drives mRNA processing in bacteria. *Proc Natl Acad Sci U S A* 2011; 108:20172-7; PMID:22123973; <http://dx.doi.org/10.1073/pnas.1113521108>.
26. Pertzev AV, Nicholson AW. Characterization of RNA sequence determinants and antideterminants of processing reactivity for a minimal substrate of *Escherichia coli* ribonuclease III. *Nucleic Acids Res* 2006; 34:3708-21; PMID:16896014; <http://dx.doi.org/10.1093/nat/gkl459>.
27. Zhang K, Nicholson AW. Regulation of ribonuclease III processing by double-helical sequence antideterminants. *Proc Natl Acad Sci U S A* 1997; 94:13437-41; PMID:9391043; <http://dx.doi.org/10.1073/pnas.94.25.13437>.
28. Felden B, Vandenesch F, Bouloc P, Romby P. The *Staphylococcus aureus* RNome and its commitment to virulence. *PLoS Pathog* 2011; 7:e1002006; PMID:21423670; <http://dx.doi.org/10.1371/journal.ppat.1002006>.
29. Gan J, Shaw G, Tropea JE, Waugh DS, Court DL, Ji X. A stepwise model for double-stranded RNA processing by ribonuclease III. *Mol Microbiol* 2008; 67:143-54; PMID:18047582; <http://dx.doi.org/10.1111/j.1365-2958.2007.06032.x>.
30. Robertson HD. *Escherichia coli* ribonuclease III cleavage sites. *Cell* 1982; 30:669-72; PMID:6754088; [http://dx.doi.org/10.1016/0092-8674\(82\)90270-7](http://dx.doi.org/10.1016/0092-8674(82)90270-7).
31. Gan J, Tropea JE, Austin BP, Court DL, Waugh DS, Ji X. Structural insight into the mechanism of double-stranded RNA processing by ribonuclease III. *Cell* 2006; 124:355-66; PMID:16439209; <http://dx.doi.org/10.1016/j.cell.2005.11.034>.
32. Blaszczyk J, Gan J, Tropea JE, Court DL, Waugh DS, Ji X. Ncatalytic assembly of ribonuclease III with double-stranded RNA. *Structure* 2004; 12:457-66; PMID:15016361; <http://dx.doi.org/10.1016/j.str.2004.02.004>.
33. Franch T, Thisted T, Gerdes K. Ribonuclease III processing of coaxially stacked RNA helices. *J Biol Chem* 1999; 274:26572-8; PMID:10473621; <http://dx.doi.org/10.1074/jbc.274.37.26572>.
34. Calin-Jageman I, Nicholson AW. Mutational analysis of an RNA internal loop as a reactivity epitope for *Escherichia coli* ribonuclease III substrates. *Biochemistry* 2003; 42:5025-34; PMID:12718545; <http://dx.doi.org/10.1021/bi030004r>.
35. Wagner EG, Altuvia S, Romby P. Antisense RNAs in bacteria and their genetic elements. *Adv Genet* 2002; 46:361-98; PMID:11931231; [http://dx.doi.org/10.1016/S0065-2660\(02\)46013-0](http://dx.doi.org/10.1016/S0065-2660(02)46013-0).
36. Brantl S. Regulatory mechanisms employed by cis-encoded antisense RNAs. *Curr Opin Microbiol* 2007; 10:102-9; PMID:17387036; <http://dx.doi.org/10.1016/j.mib.2007.03.012>.
37. Argaman L, Altuvia S. *fhlA* repression by OxyS RNA: kissing complex formation at two sites results in a stable antisense-target RNA complex. *J Mol Biol* 2000; 300:1101-12; PMID:10903857; <http://dx.doi.org/10.1006/jmbi.2000.3942>.
38. Chanfreau G, Buckle M, Jacquier A. Recognition of a conserved class of RNA tetraloops by *Saccharomyces cerevisiae* RNase III. *Proc Natl Acad Sci U S A* 2000; 97:3142-7; PMID:10716739; <http://dx.doi.org/10.1073/pnas.97.7.3142>.
39. Benito Y, Kolb FA, Romby P, Lina G, Etienne J, Vandenesch F. Probing the structure of RNAlII, the *Staphylococcus aureus* agr regulatory RNA, and identification of the RNA domain involved in repression of protein A expression. *RNA* 2000; 6:668-79; PMID:10836788; <http://dx.doi.org/10.1017/S1355838200992550>.
40. Fechter P, Chevalier C, Yusupova G, Yusupov M, Romby P, Marzi S. Ribosomal initiation complexes probed by toeprinting and effect of trans-acting translational regulators in bacteria. *Methods Mol Biol* 2009; 540:247-63; PMID:19381565; http://dx.doi.org/10.1007/978-1-59745-558-9_18.
41. Westhof E, Masquida B, Jossinet F. Predicting and modeling RNA architecture. *Cold Spring Harb Perspect Biol* 2011; 3: In press; PMID:20504963; <http://dx.doi.org/10.1101/cshperspect.a003632>.
42. Jossinet F, Ludwig TE, Westhof E. Assemble: an interactive graphical tool to analyze and build RNA architectures at the 2D and 3D levels. *Bioinformatics* 2010; 26:2057-9; PMID:20562414; <http://dx.doi.org/10.1093/bioinformatics/btq321>.